06 /SVGM/ NON-EQUILIBRIUM MARSHAK WAVE-2012

Non-Equilibrium Marshak Wave in Finite Planar Slabs using Eigen Function Expansion

S. V. G. Menon

Contact Information:

menonsvg@yahoo.co.in
menon.svg98@gmail.com

+918879394488
+918547992428

Contents

List of Figures

List of Tables

Abstract

New solutions to the non-equilibrium Marshak wave, within the Pomraning -Su-Olson model, are presented using the well known eigenfunction expansion method for finite slabs. Eigenfunctions and eigenvalues of the Helmholtz's equation satisfying the radiation boundary conditions are derived for expanding the solutions. Expansion coefficients at any order are then determined by solving two coupled first order ordinary differential equations. Numerical results for the first twenty eigenvalues and normalization constants of the eigenfunctions are given for two slab thicknesses. Further results include time dependent radiation density, material temperature, time dependent exit currents from the slab, etc. Convergence of the series for the radiation density is also established using the numerical solutions. Brief comments for extending the method to finite spherical and cylindrical geometries are given in the Appendix.

1 Introduction

Benchmark solutions to idealized problems involving radiative transfer problems have been derived in various approximations. The class of problems termed as Marshak wave propagation considers radiation incident on one side of a cold homogeneous medium and penetrating into its interior. In the original formulation of the problem, Marshak assumed that matter and radiation are in equilibrium, thereby both being characterized by a single temperature [1]. Pomraning generalized the formulation to include non-equilibrium effects, wherein radiation propagation is described by the time dependent radiation diffusion equation which is coupled to a local energy equation for the material. Considering an initially cold material, extending into a semi-infinite medium, Pomraning obtained analytical solutions to several quantities of interest assuming that the opacity of the medium is independent of temperature while its heat capacity varies as cube of temperature. Except for spatially averaged radiation energy density and material temperature, all the numerical results reported by Pomraning were within the the non-retardation approximation wherein speed of light is assumed to be infinite [2].

The model problem was considered afresh by Su and Olson who obtained results for several quantities, including spatial distributions of radiation energy density and material temperature, without invoking the non-retardation approximation [3]. These results are of great use in validating radiation diffusion codes, which are intended to solve more complex problems involving general nonlinear dependence of opacity and heat capacity on material temperature and density. Ganopal and Pomraning have also analyzed the same model problem when radiation penetration into the medium is treated using the radiation transport equation in lieu of the radiation diffusion equation [4].

In this report, the Pomraning-Su-Olson (PSO) model of Marshak wave is considered in finite sized media. Using the eigenfunction expansion (EFE) method, new benchmark results for finite slab geometry are obtained for cases of steady as well as time dependent incident radiation fluxes. It is hoped that these new results will supplement the existing data base for validating radiation diffusion computer codes [5]. The remaining part of the report is organized as follows. The Marshak wave model is explained in section 2. Specialization to planar geometry and the EFE method are covered in section 3. The first twenty eigenvalues and normalization constants of eigenfunctions for two slab thicknesses are also given in this section. All the remaining results which include time dependent radiation density, material temperature, time dependent exit currents from the slab, etc., are given in section 4. Convergence of the series for the radiation density is also established here by computing partial sums in the EFE. Extensions of the method for finite sphere and cylindrical are straightforward and are briefly indicated given in the Appendix, though no numerical results are presented. The report is concluded in section 5.

2 Marshak Wave Model

In Marshak wave propagation, radiation is incident on the left side of a homogeneous and cold medium. Within the diffusion approximation, radiation

propagation is described by

$$\frac{\partial}{\partial t}E(r,t) - cD\frac{1}{r^n}\frac{\partial}{\partial r}r^n\frac{\partial}{\partial r}E = cK(T)(\ aT^4(r,t) - E(r,t)\ ), \tag{1}$$

where $E(r,t)$ is radiation energy density at position co-ordinate r and time t. The index n takes values $0, 1$ and 2 for one dimensional planar, cylindrical and spherical geometry. The diffusion coefficient D is given by $D = 1/[3K(T)]$ where $K(T)$ denotes the gray opacity of the medium. The radiation constant a is defined as $a = 4\sigma/c$ where σ is Stefan-Boltzmann constant and c is speed of light.

Considering a boundary of the medium at r_0, the radiation flux $F_{in}(t)$ incident on the medium is specified by the Marshak boundary condition

$$\frac{1}{4}cE(r_0,t) \mp \frac{1}{2}cD\frac{\partial}{\partial r}E(r_0,t)|_{r_0} = F_{in}(t), \tag{2}$$

where the $\mp$ sign denotes radiation incident in the $\pm$ ve r-directions into the medium. A free boundary is obtained when $F_{in}(t) = 0$. The initial cold condition on radiation density is specified as $E(r,0) = 0$.

The material energy density evolves according to the local material temperature equation

$$C_v(T)\frac{\partial}{\partial t}T(r,t) = cK(T)(\ E(r,t) - aT^4(r,t)\ ), \tag{3}$$

where $C_v(T)$ is the heat capacity of the medium. The cold initial condition of the medium is further specified as $T(r,0) = 0$.

The PSO model assumes that the opacity $K(T)$ is independent of temperature and the heat capacity is given by $C_v(T) = \alpha T^3$ where α is a proportionality constant. Then the equations specifying the model can be reduced into a neat dimensionless form. For this purpose, Pomraning introduces the dimensionless independent variables [2]

$$x = \sqrt{3}\ K\ r, \quad \tau = \frac{4}{\alpha}\ a\ c\ K\ t, \tag{4}$$

and dependent variables

$$u(x,\tau) = \frac{c}{4}\frac{E}{F_0}, \quad v(x,\tau) = \frac{c}{4}\frac{a}{F_0}T^4. \tag{5}$$

Here F_0 is a normalization constant in the incident flux defined as $F_{in}(t) = F_0 f(\tau)$. Then the system of equations and boundary conditions can be cast in dimensionless form as follows:

$$\begin{aligned} \epsilon\frac{\partial}{\partial\tau}u &- \frac{1}{x^n}\frac{\partial}{\partial x}x^n\frac{\partial}{\partial x}u = v(x,\tau) - u(x,\tau) \\ \frac{\partial}{\partial\tau}v &= u(x,\tau) - v(x,\tau) \end{aligned} \tag{6}$$

$$\begin{aligned} u(x_0,\tau) &- \frac{2}{\sqrt{3}}\frac{\partial}{\partial x}u(x,\tau)|_{x_0} = f(\tau) \\ u(x_1,\tau) &+ \frac{2}{\sqrt{3}}\frac{\partial}{\partial x}u(x,\tau)|_{x_1} = 0, \end{aligned} \tag{7}$$

where $\epsilon = 4a/\alpha = 16\sigma/(c\alpha)$. The boundary at x_1 is taken to be free. The non-retardation approximation assumes that $\epsilon = 0$ and corresponds to infinite propagation speed of radition [2]. Eqs.(6) are to be solved using the boundary conditions of Eq.(7) and the initial conditions

$$u(x,0) = v(x,0) = 0 \tag{8}$$

for finite slab geometry.

2.1 Incident Radiation Flux

The case of a steady incident flux is specified by the condition $f(\tau) = 1$ (Fig.1). This was the problem considered earlier by Pomraning as well as Su and Olson [2], [3]. However, a typical time dependent incident flux (Fig.2) is also considered here for application. While this flux saturates to a steady value, there can also be problems involving a pulsed input flux, as shown in Fig.3. The method developed in this report can take into account any general time dependent input flux.

3 Eigenfunction Expansion Method

3.1 Asymptotic and Transient Solutions

For plane geometry, the transport equations reduce to the form:

$$\begin{aligned} \epsilon\frac{\partial}{\partial\tau}u &- \frac{\partial^2}{\partial x^2}u = v(x,\tau) - u(x,\tau) \\ \frac{\partial}{\partial\tau}v &= u(x,\tau) - v(x,\tau) \end{aligned} \tag{9}$$

Assuming that the slab occupies the region, $0 \le x \le b$, where b is the dimensionless thickness of the slab, the boundary conditions are given by

$$\begin{aligned} u(0,\tau) &- \frac{2}{\sqrt{3}}\frac{\partial}{\partial x}u(x,\tau)|_0 = f(\tau) \\ u(b,\tau) &+ \frac{2}{\sqrt{3}}\frac{\partial}{\partial x}u(x,\tau)|_b = 0 \end{aligned} \tag{10}$$

The initial conditions of Eq.(8) are unchanged. Solutions to Eqs.(9) can be obtained using the EFE method. However, it is necessary to restrict EFE to the part of the solution that satisfies homogeneous boundary conditions. This can be done within the PSU model as its equations are linear. So we separate the solutions $u(x,\tau)$ and $v(x,\tau)$ as

$$\begin{aligned} u(x,\tau) &= u_A(x,\tau) + u_T(x,\tau) \\ v(x,\tau) &= v_A(x,\tau) + v_T(x,\tau) \end{aligned} \tag{11}$$

where $u_A(x,\tau)$ and $v_A(x,\tau)$ are asymptotic solutions satisfying the time independent equations

$$\frac{\partial^2}{\partial x^2}u_A(x,\tau) = 0, \quad v_A(x,\tau) = u_A(x,\tau) \tag{12}$$

but same boundary conditions of Eqs.(10), viz.,

$$\begin{aligned} u_A(0,\tau) &- \frac{2}{\sqrt{3}}\frac{\partial}{\partial x}u_A(x,\tau)|_0 = f(\tau) \\ u_A(b,\tau) &+ \frac{2}{\sqrt{3}}\frac{\partial}{\partial x}u_A(x,\tau)|_b = 0 \end{aligned} \tag{13}$$

In Eqs.(12) and (13), τ is simply a parameter. Solutions to these "steady state" equations, which satisfy the boundary conditions of Eq.(13), are easily found to be

$$u_A(x,\tau) = v_A(x,\tau) = f(\tau)\frac{b + 2/\sqrt{3} - x}{b + 4\sqrt{3}} \tag{14}$$

The equations satisfied by the transient solutions $u_T(x,\tau)$ and $v_T(x,\tau)$ readily follow from substituting Eq.(11) into (9):

$$\begin{aligned} \epsilon\frac{\partial}{\partial\tau}u_T &- \frac{\partial^2}{\partial x^2}u_T = v_T(x,\tau) - u_T(x,\tau) - \epsilon\frac{\partial}{\partial\tau}u_A \\ \frac{\partial}{\partial\tau}v_T &= u_T(x,\tau) - v_T(x,\tau) - \frac{\partial}{\partial\tau}v_A \end{aligned} \tag{15}$$

These have to be solved by imposing the homogeneous boundary conditions

$$\begin{aligned} u_T(0,\tau) &- \frac{2}{\sqrt{3}}\frac{\partial}{\partial x}u_T(x,\tau)|_0 = 0 \\ u_T(b,\tau) &+ \frac{2}{\sqrt{3}}\frac{\partial}{\partial x}u_T(x,\tau)|_b = 0 \end{aligned} \tag{16}$$

and the initial conditions

$$u_T(x,0) = v_T(x,0) = -u_A(x,0) \tag{17}$$

Next a complete set of functions are obtained using the homogeneous eigenvalue problem of the Helmholtz equation. It is necessary to stress the importance of separating the solution into the asymptotic and transient parts. Functions satisfying homogeneous boundary conditions alone can be expanded in terms of the eigenfunctions, as they also usually obey homogeneous boundary conditions. Of course the Fourier functions obeying periodic boundary conditions are exceptions.

3.2 Eigenvalue Problem

Consider the eigenvalue problem

$$\frac{\partial^2}{\partial x^2}\phi(x) + \mu^2\phi(x) = 0 \tag{18}$$

with the boundary conditions

$$\begin{aligned} \phi(0) &- \frac{2}{\sqrt{3}}\frac{\partial}{\partial x}\phi|_0 = 0 \\ \phi(b) &+ \frac{2}{\sqrt{3}}\frac{\partial}{\partial x}\phi|_b = 0 \end{aligned} \tag{19}$$

The general solution to Eq.(18) can be written as

$$\begin{aligned}\phi(x) &= c\sin[\mu x + d)] \\ &= [c\cos(d)][\sin(\mu x) + \cos(\mu x)\frac{\sin(c)}{\cos(d)}] \end{aligned} \tag{20}$$

where the arbitrary constants c and d have to be determined from the boundary conditions. Application of the left boundary condition yields one condition between the arbitrary constants, viz.,

$$\frac{\sin(c)}{\cos(d)} - \frac{2}{\sqrt{3}}\mu = 0 \tag{21}$$

which is used in Eq.(20) to obtain

$$\phi(x) = C[\sin(\mu x) + \frac{2}{\sqrt{3}}\mu\cos(\mu x)] \tag{22}$$

The remaining arbitrary constant is redefined as $C = c\cos(d)$. Now, applying the right boundary condition one gets

$$\frac{2}{\sqrt{3}}\mu[\cos(\mu b) - \frac{2}{\sqrt{3}}\mu\sin(\mu b)] + [\sin(\mu b) + \frac{2}{\sqrt{3}}\mu\cos(\mu b)] = 0 \tag{23}$$

On simplification, the eigenvalue equation for determining μ is obtained as

$$\tan(\mu b) = \frac{4\mu}{4\mu^2/\sqrt{3} - \sqrt{3}} \tag{24}$$

This transcendental equation provides an infinite set of eigenvalues μ_n and the corresponding eigenfunctions

$$\phi_n(x) = C_n\sin[(\mu_n x) + (\frac{2}{\sqrt{3}}\mu_n)\cos(\mu_n x)] \tag{25}$$

The arbitrary constant C_n is determined by the normalizing condition on $\phi_n(x)$

$$\int_0^b \phi_n^2(x)dx = 1 \tag{26}$$

which provides the equation

$$C_n^2 = 12\mu_n[(3+4\mu_n^2)2\mu_n b - (3-4\mu_n^2)\sin(2\mu_n b) + 4\sqrt{3}\mu_n(1-\cos(2\mu_n b))]^{-1} \tag{27}$$

Eq.(24) shows that the roots μ_n occour in $\pm$ pairs and $\mu_n = 0$ is a root. Further its RHS decreases as μ_n^{-1} for large n, and hence the asymptotic eigenvalues values are separated by π. The first twenty positive eigenvalues and normalization constants for $b = 1$ and $b = 5$ are listed in Table 1. The eigenfunctions given in Eq.(25) are now orthonormal for different positive eigenvalues:

$$\int_0^b \phi_n(x)\phi_m(x)dx = \delta_{mn} \tag{28}$$

Table 1: Eigenvalues μ_n and normalization constants C_n

$No.$	μ_n $b=1$	C_n $b=1$	μ_n $b=5$	C_n $b=5$
1	1.22826	0.613088	0.440209	0.482207
2	3.61221	0.310784	1.46964	0.30353
3	6.54624	0.181898	2.04518	0.238385
4	9.60463	0.125863	2.64006	0.192851
5	12.7025	0.0956844	3.24589	0.160594
6	15.8174	0.0770492	3.85823	0.137006
7	18.9409	0.0644387	4.47470	0.119185
8	22.0696	0.0553538	5.09391	0.105323
9	25.2014	0.0485035	5.71502	0.0942699
10	28.3354	0.0431565	6.33751	0.0852695
11	31.4709	0.0388681	6.96101	0.0778089
12	34.6076	0.0353528	7.58529	0.0715302
13	37.7450	0.0324296	8.21018	0.0661766
14	40.8831	0.029935	8.83554	0.0615601
15	44.0216	0.0278037	9.46129	0.0575396
16	47.1600	0.0259552	10.0874	0.0540078
17	50.2999	0.0243369	10.7137	0.0508812
18	53.4395	0.0229084	11.3402	0.0480945
19	56.5793	0.0216381	11.9669	0.0455954
20	59.7193	0.0205012	12.5938	0.0433418

where δ_{mn} is the Kronecker delta. The first three eigenfunctions for slab thickness $b = 1$ are shown in Fig.4. It is important to realize that a complete set of eigenvalues and eigenfunctions have to be determined for the EFE method as outlined above. For example, a simple Fourier expansion will not suffice since that will not satisfy the boundary conditions on the radiation density.

3.3 Series Solution

The eigenfunctions form a complete set and the transient solutions $u_T(x,\tau)$ and $v_T(x,\tau)$, which satisfy homogeneous boundary conditions, can be expanded as

$$\begin{aligned} u_T(x,\tau) &= \sum_{n=1}^{\infty} a_n(\tau)\phi_n(x) \\ v_T(x,\tau) &= \sum_{n=1}^{\infty} b_n(\tau)\phi_n(x) \end{aligned} \tag{29}$$

The expansion is restricted to positive values of μ_n as the the transient solutions should tend to zero for large τ. Subsitution into Eqs.(15) gives a set of ordinary differential equations (ODE):

$$\begin{aligned} \epsilon \dot{a_m} &+ a_m(\mu_m^2 + 1) - b_m = -\epsilon f'(\tau) g_n \\ \dot{b_m} &+ b_m - a_m = -f'(\tau) g_n \end{aligned} \tag{30}$$

where $f'(\tau)$ is the derivtive of $f(\tau)$ with τ and g_n is given by

$$g_n = \int_0^b \phi_n(x) \frac{b + 2/\sqrt{3} - x}{b + 4\sqrt{3}} dx \tag{31}$$

The initial conditions on $a_n(\tau)$ and $b_n(\tau)$, obtained by using Eqs.(29) in Eq.(17) and the orthogonality of the eigenfunctions, are given by

$$a_n(0) = b_n(0) = -g_n \tag{32}$$

The set of ODE in Eq.(30) can be readily integrated using the initial conditions given above.

4 Results

First of all, consider the case of a constant incident flux. Spatial distribution the radiation density ($u(x,\tau)$) for slab thickness $b = 1$ are shown in Fig.5 for four values of τ, viz., 0.01, 0.1, 1 and 10. The asymptotic solution, also shown there, almost coincides with the solution at $\tau = 10.$, thereby showing that a steady state is reached by this time for the case of constant input flux.

For the case of rising incident flux (Fig.2), spatial distributions of the radiation density, $u(x,\tau)$, and material temperature, $v(x,\tau)$, are shown in Fig.6 for three values of τ; 3, 5 and 10. Initially, $v(x,\tau)$ lags behind $u(x,\tau)$, however it catches up later. It should be noted that $v(x,\tau) \sim T^4(x,\tau)$, and hence $T(x,\tau)$

Table 2: Convergence of eigenfunction expansion $u_T(b/2, \tau, N)$

N	$\tau = 3$	$\tau = 5$	$\tau = 8$
1	0.106457	0.358914	0.470546
2	0.106457	0.358914	0.470546
3	0.106971	0.359123	0.470557
4	0.106971	0.359123	0.470557
5	0.106932	0.359108	0.470556
6	0.106932	0.359108	0.470556
7	0.10694	0.359111	0.470556
8	0.10694	0.359111	0.470556
9	0.106938	0.35911	0.470556
10	0.106938	0.35911	0.470556

would have more steeper spatial distribution. The first two coefficients in the series expansion of $u(x, \tau)$ and $v(x, \tau)$ are shown in Fig.7. The characteristic feature in their variation is the initial build up and later decay to zero as required for the transient solution for the rising incident flux. The exit currents; i.e., the currents leaving the left and right surfaces, are given by:

$$\begin{aligned} j_-(0, \tau) &= u(0, \tau) + \frac{2}{\sqrt{3}} \frac{\partial}{\partial x} u(x, \tau)|_0 \\ j_+(b, \tau) &= u(b, \tau) - \frac{2}{\sqrt{3}} \frac{\partial}{\partial x} u(x, \tau)|_b \end{aligned} \tag{33}$$

Their time dependence is shown in Fig.8. A negative value of $j_-(0, \tau)$ up to $tau \sim 5$ indicates that no radiation is leaving the left surface during this time.

All the results discussed above were obtained with $N = 20$. To test the convergence of the series in the EFE method, we next calculate partial sums for the radiation density:

$$u_T(x, \tau, N) = \sum_{n=1}^{N} a_n(\tau) \phi_n(x) \tag{34}$$

These are tabulated in Table 2 for different values of N at $x = b/2$ and $\tau = 3, 5, 8$. It is clear that the results converge quite well as N is increased up to about 10. However, more terms would be needed for slabs of larger thicknesses.

5 Conclusions

In this report we have presented the EFE method to solve the Marshak wave propagation problem in finite slabs within the PSO model. Numerical results for the eigenvalues and normalization constants, time dependent radiation density, material temperature, exit currents, etc., have been provided. Convergence of

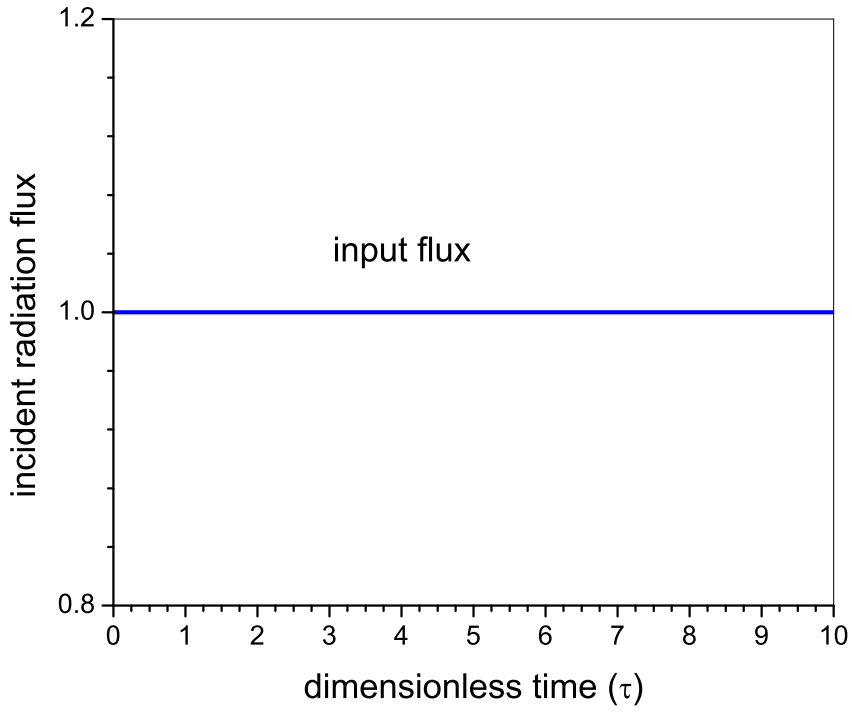

Figure 1: Constant incident radiation flux $f(\tau)$ Vs time (τ)

the expansion has also been shown. The attractive feature of the method is that any quantity depending on the radiation density or material temperature can be easily computed. Further, general time dependent incident flux, as may occur in experiments, can also be incorporated. the method can be generalized to other one dimensional geometries.

References

[1] R. E. Marshak, Phys. Fluids, 1, 24, 1958.

[2] G. C. Pomraning, J. Quant. Spec. Rad. Tranf., 21, 249, 1979.

[3] O. Su and G. L. Olson, J. Quant. Spec. Rad. Tranf., 56, 337, 1996.

[4] B. D. Ganopal and G. C. Pomraning, J. Quant. Spec. Rad. Tranf., 25, 325, 1981.

[5] Diffusion and Multi-Angle radiation transport models, www.prism-cs.com/Helios/HELIOS - radiation - transport - benchmarks.

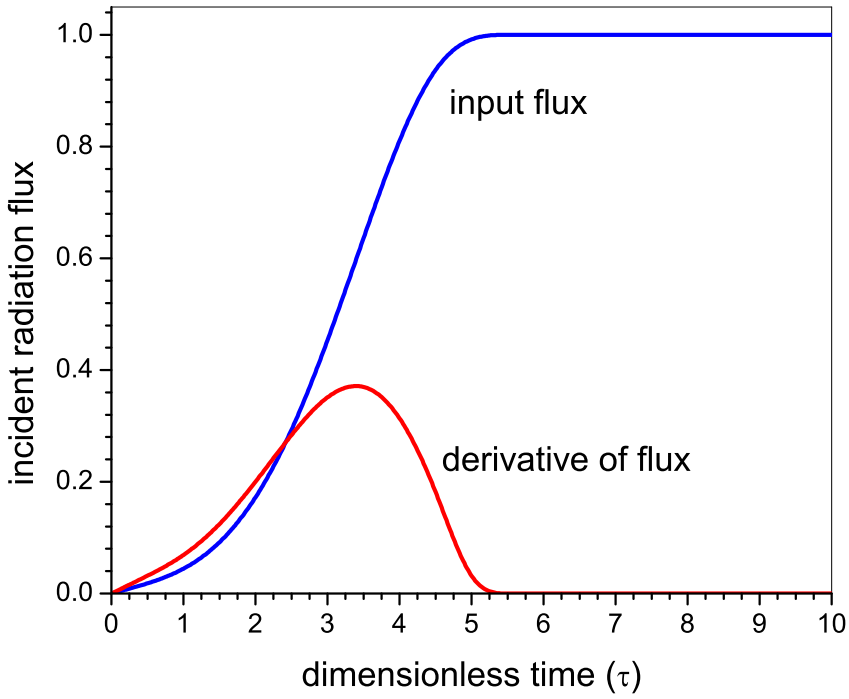

Figure 2: Rising incident radiation flux $f(\tau)$ Vs time (τ)

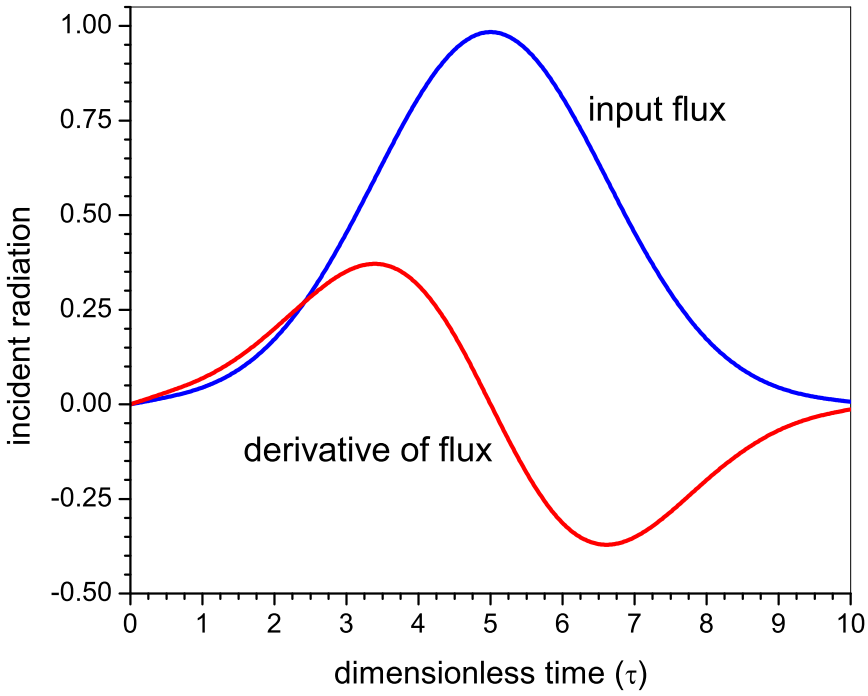

Figure 3: Gaussian incident radiation flux $f(\tau)$ Vs time (τ)

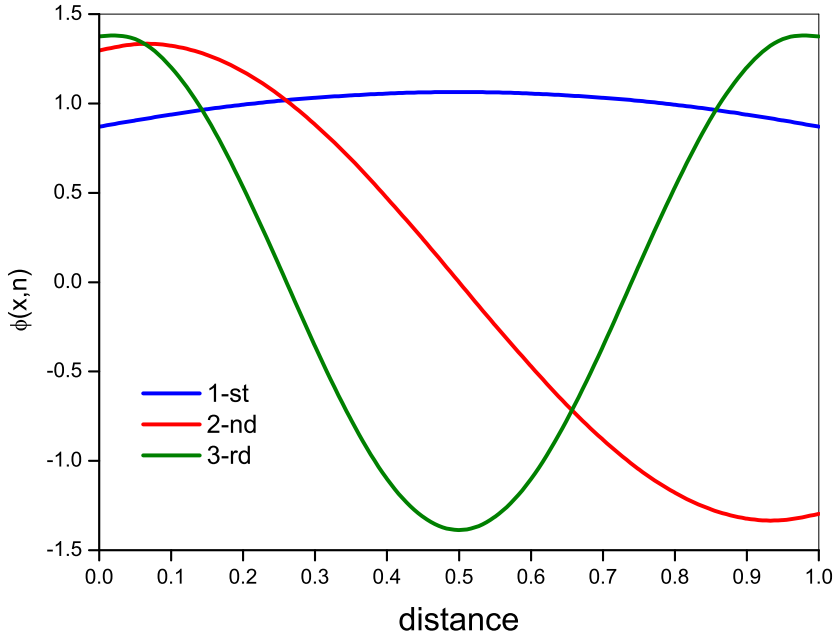

Figure 4: Eigenfunctions $\phi_n(x)$ Vs distance (x)

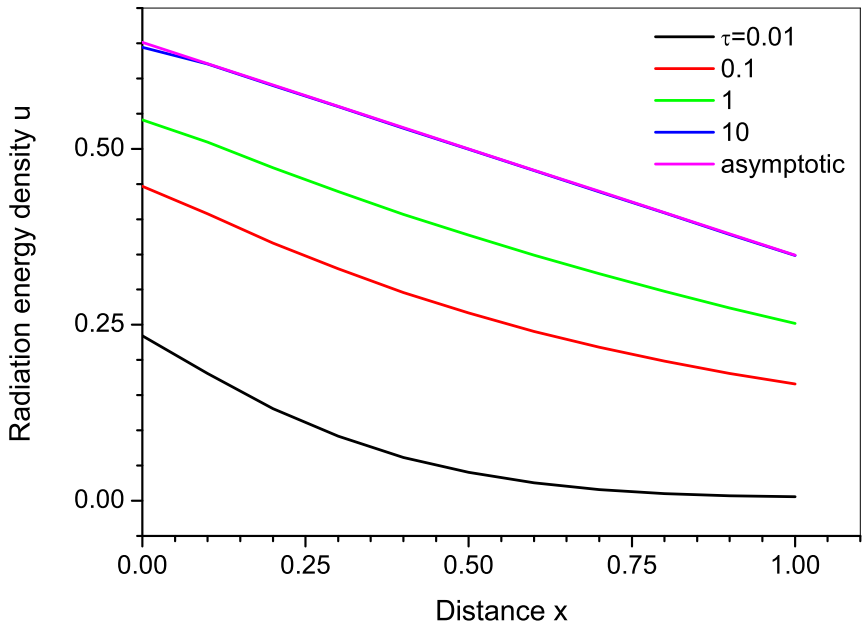

Figure 5: Radiation energy density $u(x, \tau)$ for thickness b=1 and constant incident flux, and $u_A(x)$

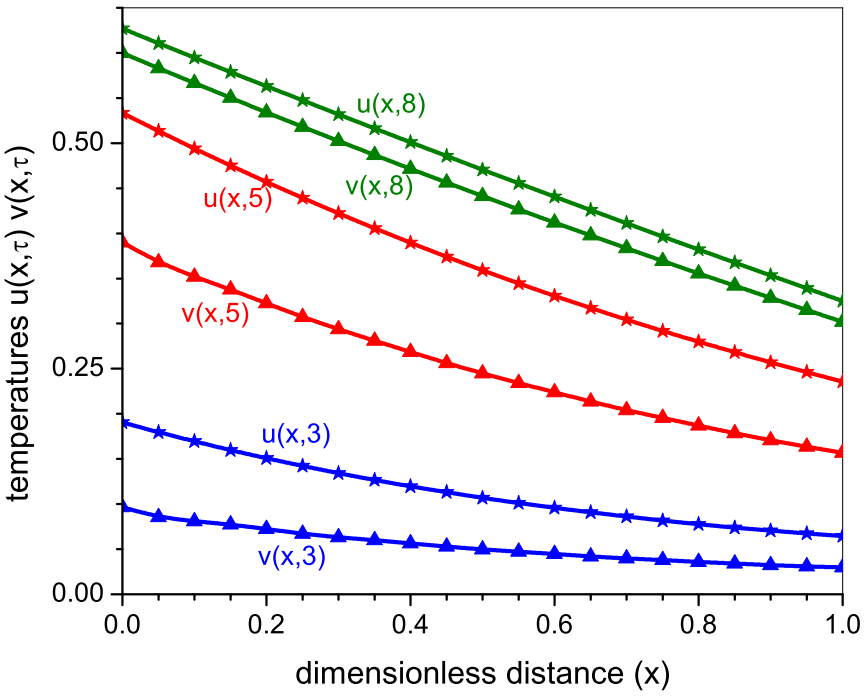

Figure 6: Radiation energy density $u(x,\tau)$ and temperature $v(x,\tau)$ for thickness b=1 and rising incident flux

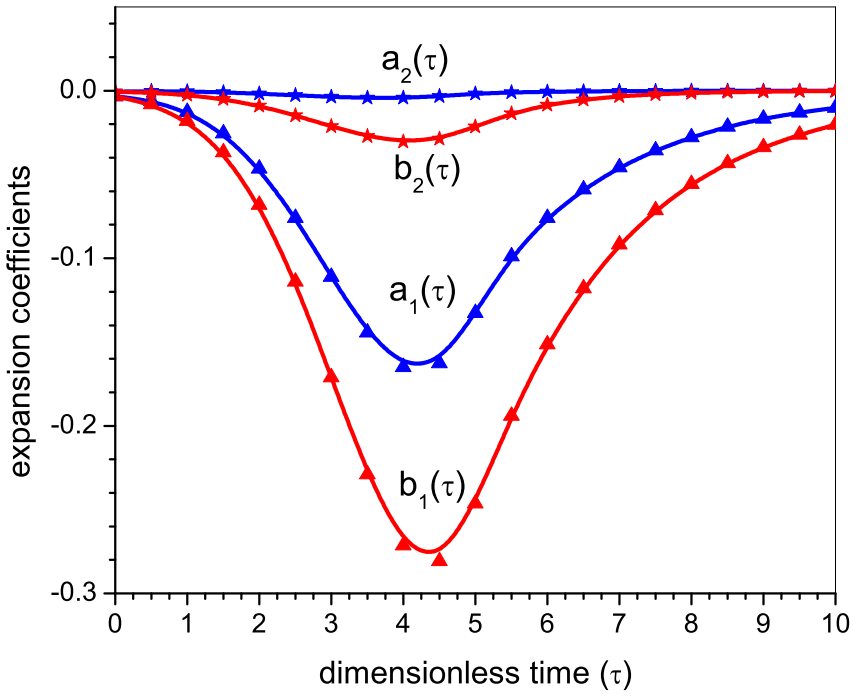

Figure 7: Expansion coefficients $a_1(\tau), b_1(\tau), a_2(\tau), b_2(\tau)$ Vs time (τ)

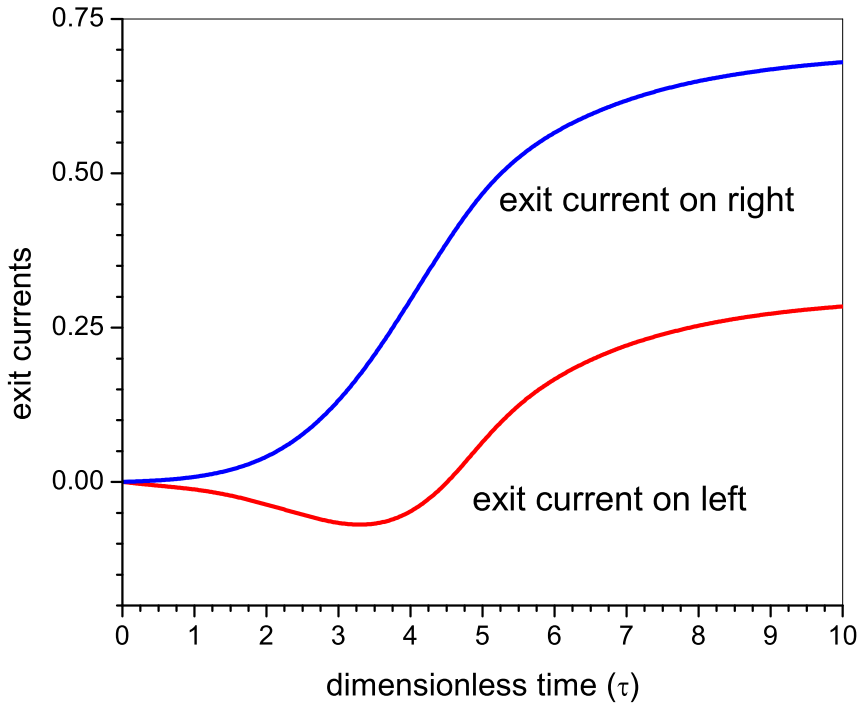

Figure 8: Exit currents $j_-(0,\tau)$ and $j_+(b,\tau)$ Vs time (τ)

A Spherical and Cylindrical Geometries

The EFE method described in the main text can be generalized to spherical and cylindrical geometries in a straightforward manner with minor modifications in the boundary conditions. For example, in the cases of finite sphere or cylinder, the incident radiation would be on the outer boundary. For spherical geometry, the eigenvalue equation is

$$\frac{1}{x^2}\frac{\partial}{\partial x}x^2\frac{\partial}{\partial x}\phi(x) + \mu^2\phi(x) = 0 \tag{35}$$

which can be reduced to that in planar case with the substitution $\phi(x) = \psi(x)/x$. The boundary condition on $\phi(x)$ at the right boundary is same as that in planar geometry. However, boundary condition to be used at the centre is that $\phi(0)$ is finite.

For spherical or cylindrical shells, the situation is almost identical to that for planar slabs. The differences in the spatial derivative terms in the diffusion equation and the volume elements shound be noted. Thus the method can be used to study equilibration and decay of a radiation pulse in a spherical or cylindrical shell thereby simulating a laser driven hohlraum.